JOURNAL OF CATALYSIS 130, 192–201 (1991)

An EXAFS Study of the Spreading of MoO_3 on the Surface of γ-Al_2O_3

GÁBOR KISFALUDI,*[,1] JÜRGEN LEYRER,†[,2] HELMUT KNÖZINGER,† AND ROEL PRINS*

*Technisch-Chemisches Laboratorium, ETH Zürich, Universitätstrasse 6, 8092 Zürich, Switzerland; and †Institut für Physikalische Chemie, Universität München, Sophienstrasse 11, 8000 München 2, Germany

Received January 26, 1990; revised February 11, 1991

An EXAFS analysis has been carried out of physical mixtures of MoO_3 with γ-Al_2O_3 prior to and after thermal treatment at 720 K in the absence and presence of water vapor. The degree of order in the MoO_3/Al_2O_3 samples decreases during calcination. This loss of long-range order is even more pronounced in the presence of water vapor than in its absence. The local order around molybdenum after thermal treatment in a dry atmosphere still resembles that in MoO_3, while significant structural modifications are induced when water vapor is present. After calcination a new Mo–*X* distance was observed which may correspond to a Mo–Al contribution in a Mo–O–Al configuration. The EXAFS results support earlier conclusions from ion scattering and Raman spectroscopy studies on identical samples, which suggests a spreading of MoO_3 over the surface of alumina as a result of solid–solid wetting. © 1991 Academic Press, Inc.

INTRODUCTION

Alumina-supported molybdenum-based materials are extensively used in the petroleum industry as catalyst precursors in hydrotreating processes (*1*). Typically this class of catalytic materials is prepared by impregnation of the support with an aqueous solution of ammonium heptamolybdate, $(NH_4)_6Mo_7O_{24}$. Xie and co-workers first demonstrated in a series of papers (*2–4*) that the calcination of a physical mixture of polycrystalline MoO_3 and γ-Al_2O_3 (and other support oxides) in air at temperatures near 700 K led to the disappearance of the X-ray diffraction pattern of MoO_3. This was interpreted as monolayer dispersion of MoO_3 on γ-Al_2O_3. X-ray photoelectron spectroscopy provided supporting results for this interpretation. Stampfl *et al.* (*5*) followed the calcination in air of MoO_3 mixed with various support oxides by laser Raman and infrared spectroscopy. They also reported indications for monolayer dispersion on Al_2O_3. Spreading was also observed by Haber *et al.* (*6, 7*) in a variety of oxide combinations and Ziólkowski and co-workers (*8, 9*) have stressed the importance of this phenomenon for solid-state reactions.

We have recently reported in a series of papers (*10–13*) that dispersed supported MoO_3/Al_2O_3 (and other) catalysts can be obtained from physical mixtures by spreading of MoO_3 on the surface of the alumina support. It has been demonstrated that water vapor plays a crucial role in chemical transformations that occur during the spreading process. Ion scattering spectroscopy (ISS) clearly showed (*11, 13*) that the molybdenum oxide covered the alumina surface in the presence and absence of water vapor. Laser Raman spectra suggested (*10, 11, 13*) that the surface phase after spreading in a water-free oxygen atmosphere was structurally similar (if not identical) to MoO_3, whereas a surface polymolybdate, probably a heptamolybdate, formed in the presence of water vapor. This latter species is considered to be structurally identical to that found in conventionally impregnated materials

[1] Permanent address: Institute of Isotopes, Hungarian Academy of Sciences, P.O. Box 77, H-1525 Budapest, Hungary.

[2] Present address: Degussa Wolfgang, 6450 Hanau, Germany.

0021-9517/91 $3.00

and develops identical activity for thiophene hydrodesulfurization (*1*, *14*). Very recently we demonstrated by Raman microscopy (*15*) that the transport of MoO_3 on Al_2O_3 surfaces occurs over macroscopic distances, i.e., several hundred micrometers under the experimental conditions applied. Gas-phase transport and surface diffusion in a concentration gradient could almost certainly be excluded as operating transport mechanisms. Solid–solid wetting is therefore considered to be responsible for the spreading phenomenon.

In the present contribution we report additional evidence for the phenomena described earlier, which was obtained by EXAFS measurements on samples prepared under conditions identical to those applied in earlier studies (*10–15*).

EXPERIMENTAL

Sample Preparation

γ-Al_2O_3 was prepared by calcination of the hydroxide (PURAL SB, Condea) in air at 1048 K for 24 h. The resulting oxide has an N_2-BET surface area of 123 m^2g^{-1}. MoO_3 was a Merck product (AR grade). The physical mixture (MOFM) was prepared by first tumbling a portion of γ-Al_2O_3 and an amount of 7.6 wt% MoO_3. This mixture was hand-ground in an agate mortar for 20 min. Quantities of this powder were placed into a quartz reactor for heat treatments in controlled atmospheres. A stream of dry argon (0.83 cm^3/s) was passed through the reactor during the initial warm-up period. When the final temperature of 720 K was reached, an O_2 flow (0.83 cm^3/s) was admitted either dry or saturated with water vapor (3.2 kPa) for 30 h. After this treatment, O_2 was replaced by Ar and the sample was allowed to cool to room temperature. The dry calcined sample is denoted MODO, and the one calcined in the presence of water vapor MOWO. The EXAFS samples consisted of self-supporting wafers, pressed from the powdered materials with a thickness such that the X-ray absorbance $\mu x = 2.5$. The samples were placed in an *in situ* EXAFS cell flushed with helium and were cooled to 77 K.

EXAFS Analysis

The EXAFS measurements were performed at 77 K on Wiggler-station 9.2 at the Synchrotron Radiation Source in Daresbury (England) with a beam of 2 GeV, 210–230 mA, and with 50% higher harmonic rejection. Using the single scattering approximation, the EXAFS phenomenon can be described by

TABLE 1

Parameters Used in the Evaluation of the Mo–Mo and Mo–O Phase Shift and Backscattering Amplitude Functions from the MoS_2 and $Na_2MoO_4.2H_2O$ Reference Compounds, and the k Ranges Used in the Analysis of the MOFM, MODO, and MOWO Samples

Sample	Contribution	N	R(Å)	Fourier-transformation range			
				Forward		Inverse	
				k_{min}(Å^{-1})	k_{max}(Å^{-1})	R_{min}(Å)	R_{max}(Å)
MoS_2	Mo—Mo	6	3.16[a]	3.16	24.48	2.40	3.22
Na_2MoO_4	Mo—O	4	1.772[b]	3.40	14.80	0.45	1.90
MOFM				4.47	13.33		
MODO				4.95	12.59		
MOWO				3.79	14.58		

[a] Ref. (*16*).
[b] Ref. (*17*).

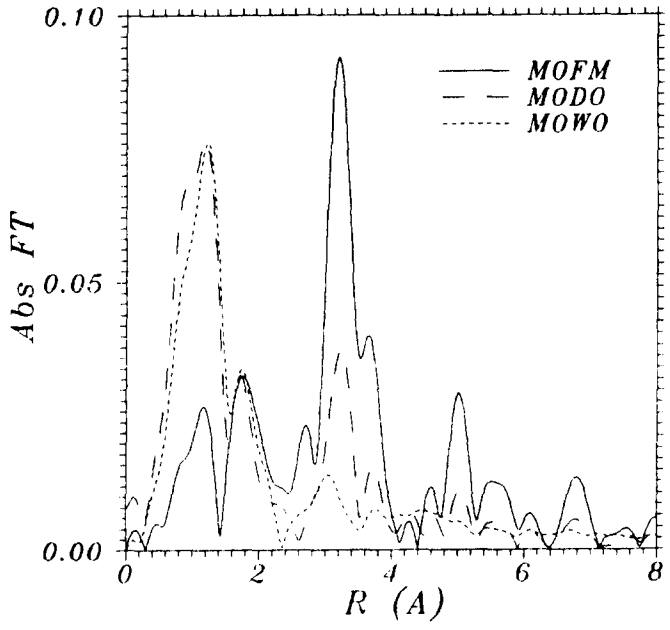

FIG. 1. Absolute part of the uncorrected k-weighted Fourier transforms of the EXAFS spectra of the MoO_3/Al_2O_3 physical mixture (MOFM), and of the dry (MODO) and the wet (MOWO) calcined samples.

$$\chi(k) = \sum_j N_j/kR_j^2 \cdot S_0(k) \cdot F_j(k) \cdot \exp(-2k^2\sigma^2) \cdot \exp(-2(R_j - \Delta)/\lambda) \cdot \sin(2kR_j + \phi_j(k)),$$

where N_j and R_j are the coordination number and distance of the atoms in the jth shell surrounding the atom which undergoes photoionization, $k = (8m/h^2(E - E_0))^{1/2}$ is the electron wave vector, $E - E_0$ is the kinetic energy of the outgoing electron, $S_0(k)$ is the shake-up factor, $F_j(k)$ is the backscattering amplitude function, $\exp(-2k^2\sigma^2)$ is the Debye–Waller thermal and structural disorder term, λ is the mean free path of the outgoing electron (set to 5 Å in all our analyses), Δ is the coordination distance of the atoms in the first coordination shell, and $\phi_j(k)$ is the phase function of the jth shell. The backscattering amplitude and phase functions for the Mo–Mo and Mo–O contributions were obtained from the EXAFS spectra of MoS_2 and $Na_2MoO_4 \cdot 2H_2O$, respectively, both measured *in vacuo* at 77 K. The coordination numbers and distances used in the analysis of the reference compounds are given in Table 1 (*16, 17*). The EXAFS analysis was performed by fitting in k space and by using the file difference technique (*18*). The contributions in the Fourier transforms of the EXAFS spectra of the MoO_3–Al_2O_3 samples were modeled up to 4 Å and the data ranges considered in the analysis are given in Table 1.

RESULTS

In order to monitor the structural differences between the three MoO_3-Al_2O_3 samples, it is worthwhile to look at the k-weighted Fourier transforms ($\psi^{nc}(R)$), which have not been corrected (*18*) for the k-dependence of $F(k)$ and $\phi(k)$ (Fig. 1). The Fourier transformations have been made between 3.74 and 13.26 $Å^{-1}$ for this purpose. The peaks in the $\psi^{nc}(R)$ plot represent scattering contributions of neighboring atoms which are present at certain distances, while the peak heights are dependent on their coordination numbers and Debye–Waller factors. Comparison of the three Fourier transforms shows that the physical mixture has

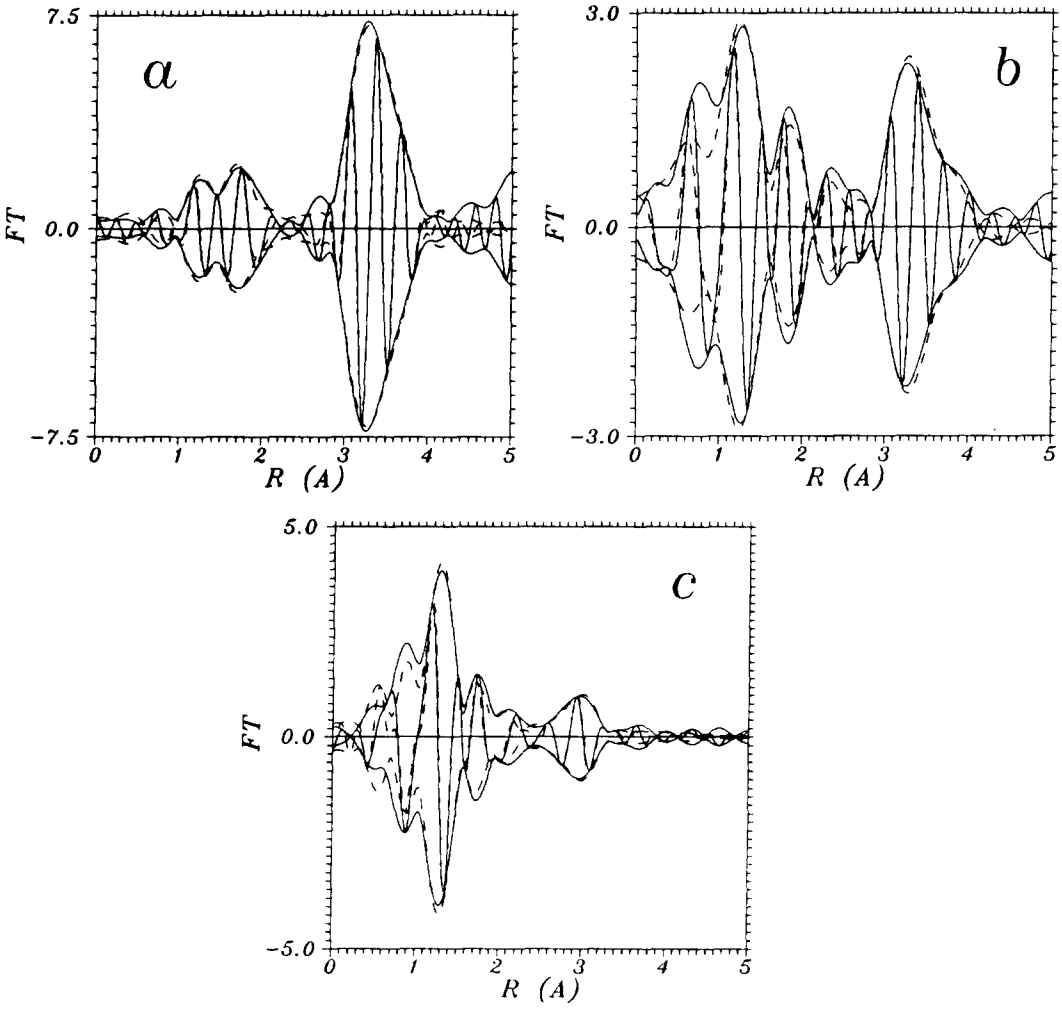

FIG. 2. Absolute and imaginary parts of the uncorrected k^3-weighted Fourier transforms for the EXAFS for the MoO_3/Al_2O_3 physical mixture (a), of the dry (b) and the wet (c) calcined samples (solid line), and the corresponding models (dashed line).

a regular structure even at long range, whereas the dry calcined sample and especially the wet calcined one show only short-range order. The k^3-weighted $\psi^{nc}(R)$ Fourier transforms of the EXAFS spectra of the three samples and the corresponding fits of the data analysis are plotted in Fig. 2. Table 2 contains the results of the data analysis for the physical mixture (MOFM), for the dry (MODO), and for the wet calcined (MOWO) samples after phase and amplitude corrections. The region of R = 1.5–2.5 Å was difficult to analyze and no unequivocal result could be obtained. Since the physical mixture contains pure MoO_3, we have assumed in the analysis of the MOFM spectrum that all crystallographically known distances of MoO_3 (*19, 20*) are present in this region of the MOFM spectrum, but we have kept the coordination numbers as free parameters in the fitting analysis. The resulting coordination numbers of 0.1, 0.6, 1.4, 0.01, and 1.8 for the 1.5–2.5 Å range (Table 2) are to be compared with the crystallographic

TABLE 2

EXAFS Results of the MoO_3–Al_2O_3 Physical Mixture Without Calcination (MOFM), the Same Mixture after Additional Dry Calcination for 30 h in O_2 (MODO), and of the Mixture after Calcination for 30 h in O_2 and H_2O (MOWO)

Contribution	N_{corr}	R (Å)	$10^4 \times \Delta\sigma^2$(Å^2)	ΔE_0(eV)
		MOFM		
Mo–O(1)	0.1	1.67[a]	−57	0
Mo–O(2)	0.6	1.73[a]	−6	0
Mo–O(3)	1.4	1.95[a]	30	5
Mo–O(4)	0.01[b]	2.25[a]	−150	0
Mo–O(5)	1.8	2.33[a]	18	−5
Mo–O(6)	3.7	3.31	−45	16
Mo–O(7)	5.7	3.89	−51	2
Mo–Mo(1)	9.2	3.44	60	3
Mo–Mo(2)	9.0	4.05	113	8
		MODO		
Mo–O(1)	1.5	1.70	5	8
Mo–O(2)	0.6	2.26	−21	15
Mo–X(3)[c]	0.5	2.78	3	2
Mo–O(4)	0.7	3.29	−53	14
Mo–O(5)	1.8	3.86	−41	11
Mo–Mo(1)	7.5	3.46	140	2
Mo–Mo(2)	2.0	4.03	42	16
		MOWO		
Mo–O(1)	1.4	1.71	−2	10
Mo–O(2)	3.0	2.40	140	−12
Mo–X(3)[c]	1.8	2.79	237	−19
Mo–O(4)	1.3	3.40	−31	−6
Mo–Mo(1)	0.5	3.31	14	11

[a] These distances were kept fixed to the crystallographic distances (*17*) in the EXAFS analysis.
[b] See Results for a discussion of this low number.
[c] In the analysis X was assumed to be an oxygen atom. See the Discussion for further details.

numbers of 1, 1, 2, 1, and 1, respectively (*20*). The Mo–O(4) coordination at 2.25 Å has an unrealistically low coordination number of 0.01, whereas the nearby Mo–O(5) coordination at 2.33 Å has a too high coordination number of 1.8. However, the sum of these two contributions is reasonably well fitted. It is clear that the fit in the 1.5 to 2.5-Å region is not very good. This was to be expected, however, since low k values cannot be used in the plane wave approximation and the backscattering amplitude of oxygen decreases strongly at high k values, limiting the Mo–O analysis to a narrow k range (*21*). This effect is most important for compounds such as MoO_3 which have an irregular structure with slightly differing distances. It leads to an apparent loss of coordination numbers, as previously observed by Chiu *et al.* for a series of oxidic Mo compounds (*22*).

The upper R region (R = 3.0–4.1 Å) of all three samples could be analyzed without any assumption. The results are presented in Table 2. Above 3 Å the distances and coordination numbers may have been influenced by multiple scattering, but the data can nevertheless be used in a qualitative sense.

DISCUSSION

The results of the EXAFS study support the conclusions that have been drawn from

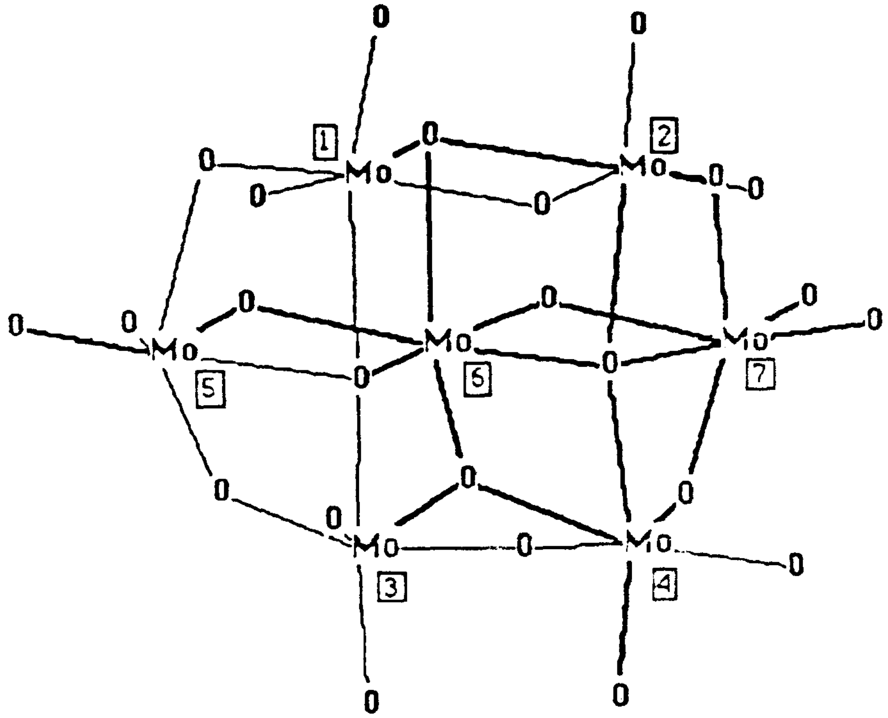

FIG. 3. Structure of the $Mo_7O_{24}^{6-}$ ion. The numbers in the squares identify the Mo atoms as used in Fig. 4.

ISS and Raman spectroscopy (*10–13*). The idea of spreading is confirmed, because the noncalcined physical mixture has a long-range order, whereas only a short-range order was found in the other two samples. The loss of order is reflected in a significant decrease of the molybdenum and oxygen coordination numbers (see Table 2). Since electron microscopy measurements demonstrated MoO_3 crystallites to be present in the MODO sample (*23*), the dry calcination apparently leads to an inhomogeneous Mo distribution. The change in the structure during wet calcination is also confirmed, because the Mo–Mo distances (3.31 Å) are significantly different in the wet calcined sample from that in the physical mixture and in the dry calcined sample (3.44–3.46 Å). In addition to these qualitative conclusions, it would be desirable to identify the distances which are present in the samples, in order to obtain an idea about the species which are effective in the wetting process. The maximum amount of information that can be obtained from an EXAFS spectrum is limited, however, by the Brillouin equation, which states that the number of parameters that can be determined is equal to $2\,\Delta R\,\Delta k/\pi$, where $\Delta k \equiv k_{max} - k_{min}$, i.e., the data region to be analyzed and $\Delta R \equiv R_{max} - R_{min}$, i.e., the distance region in which the contributions are situated. For instance, since each contribution in the EXAFS spectrum is determined by four parameters (N, R, $\Delta\sigma^2$, and ΔE_0), this means that for the MOWO sample (with Δk = 10.97 Å^{-1}) a ΔR range of 1.15 Å is needed to be able to determine two contributions. The Brillouin condition gives the possibility to estimate which compounds can be fully analyzed. As a rule of thumb, compounds in which the atoms are not at positions of high symmetry and whose elementary cells contain more than one atom of the same element have

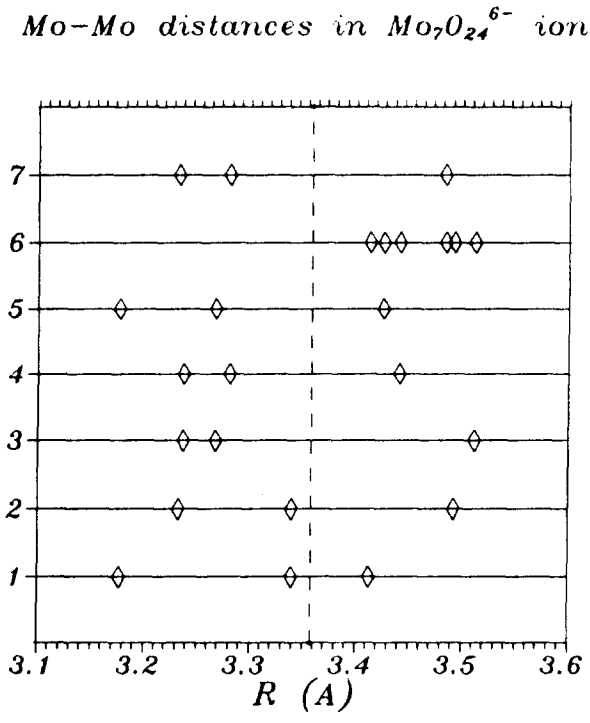

FIG. 4. Mo–Mo distances in the $Mo_7O_{24}^{6-}$ ion. The numbering on the vertical axis refers to the Mo atoms as indicated in Fig. 3.

groups of slightly different atomic distances. This leads to ambiguity in the analysis.

As a case in point, consider the heptamolybdate ion ($Mo_7O_{24}^{6-}$), which may have been formed during wet calcination. Its structure and the corresponding 24 Mo–Mo distances (*19*) are given in Figs. 3 and 4, respectively. An EXAFS spectrum was synthesized by using the Mo–Mo reference and these 24 Mo–Mo crystallographic distances in the region of 3.1–3.6 Å with the assumption that $\Delta\sigma^2 = 0$ and $\Delta E_0 = 0$ for each Mo–Mo contribution. Thereafter, this spectrum was analyzed in the same way as were our samples. The range of the Fourier transformation was $k = 3.60 - 14.57$ Å^{-1}. The parameters from the fit are given in Table 3 and the k^3-weighted Fourier transforms for both the synthetic spectrum and the model made from the fit are plotted in Fig. 5. It is remarkable that the 24-contribution model can be described perfectly by two contributions even though there are six coordinations missing ($\Sigma N_{corr} = 18$ in Table 3). As previously in the analysis of the 1.5–2.5 Å region of the MOFM spectrum, this decrease in the coordination number is caused by the addition of sine functions of different phases, which may result in an increase as well as a decrease in the overall amplitude (*21*). It is obvious that the result would be

TABLE 3

EXAFS Results for a 24-Contribution Model of $Mo_7O_{24}^{6-}$

Contribution	N_{corr}	R (Å)	$10^4 \times \Delta\sigma^2$ (Å^2)	ΔE_0 (eV)
Mo–Mo(1)	8.6	3.25	16	2
Mo–Mo(2)	9.4	3.47	12	−2

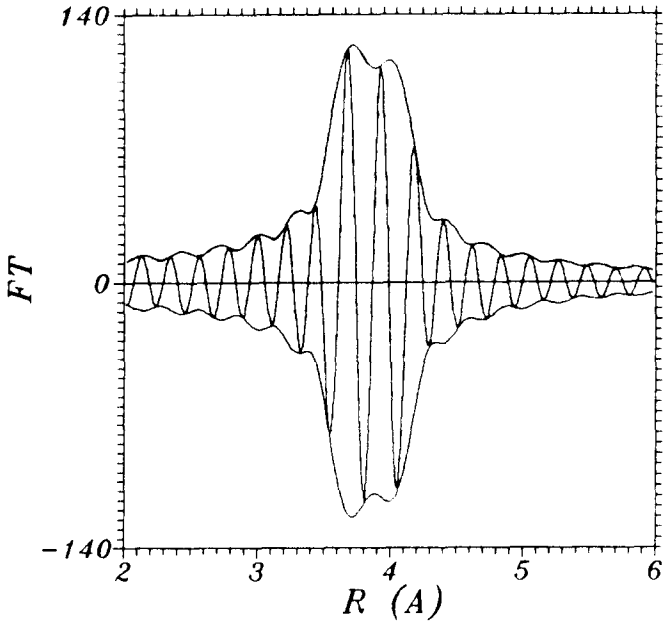

FIG. 5. k^3-Weighted Fourier transforms of the 24-Mo–Mo-contribution synthesized spectrum and of the fitted two Mo–Mo-contribution model (both Fourier transforms completely overlap over the full range). Both Fourier transforms are corrected for Mo–Mo phase shift and backscattering amplitude functions.

ambiguous if more than these two contributions were analyzed within this ΔR region. This conclusion is in accordance with the conclusion from the Brillouin equation.

In spite of this difficulty of not being able to estimate how many real contributions are present, it is still worthwhile to compare the EXAFS results of the MoO_3/Al_2O_3 with those of some model compounds. Figure 6 shows our measured Mo–O distances (lower part of the plot), as well as the Mo–O distances up to 4 Å calculated from the XRD data for MoO_3 (*20*), $(NH_4)_6Mo_7O_{24}$ and for $Al_2(MoO_4)_3$ (*24*) (upper part). Since the unit cells of the molybdates contain several molybdenum atoms in different positions, the distances belonging to a particular Mo position are presented on the same horizontal line. This plot demonstrates that the distance of about 2.8 Å as observed in the calcined samples does not correspond to any Mo–O distance in the model compounds. This contribution is well separated from the others (i.e., it fulfills the criterion from the Brillouin equation), and therefore it is considered real. The assignment of this distance around 2.8 Å to a Mo–O contribution is open to discussion. It might also be due to a Mo–Al contribution in a Mo–O–Al configuration. In that case, however, the structural data for this contribution as given in Table 2 are not correct, since the $F(k)$ and the $\phi(k)$ functions for Mo–O and Mo–Al contributions are different (*25*). Furthermore, in that case the data for the other contributions will not be correct either, since all contributions interfere in k space. This means that the fitting procedure should be repeated with the appropriate $F(k)$ and the $\phi(k)$ functions obtained from a Mo–Al reference. Nevertheless, the outcome is still appropriate for a qualitative consideration such as we have made so far, since the phase and the amplitude functions of the Mo–O and Mo–Al contributions differ only slightly (*25*).

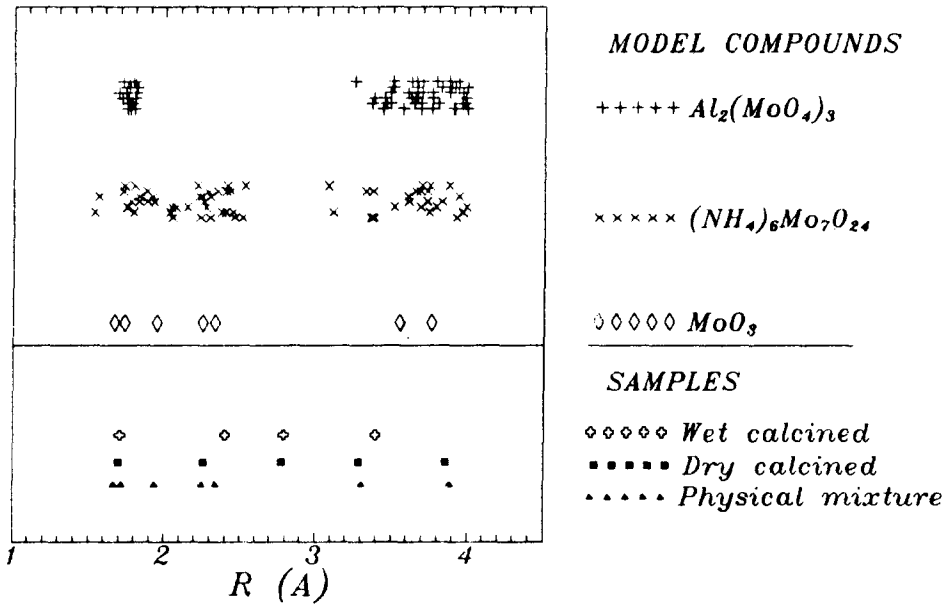

FIG. 6. The Mo–O distances obtained from the analyses of the three samples (lower part) and from the crystallographic data of $Al_2(MoO_4)_3$, $(NH_4)_6Mo_7O_{24}$, and MoO_3 (upper part).

CONCLUSIONS

The present EXAFS results suggest a dramatic loss of long-range order of MoO_3 when physical mixtures of MoO_3 and γ-Al_2O_3 are thermally treated at 720 K, as indicated particularly by the decrease in Mo–Mo coordination numbers (see Table 2). The decrease in the Mo–Mo coordination number is even more pronounced in the presence of water vapor during thermal treatment than in its absence. This observation can be interpreted as a spreading of the MoO_3 over the surface of γ-Al_2O_3 and is thus consistent with conclusions drawn earlier from ion scattering spectroscopy (*11*, *13*). The local order around molybdenum after thermal treatment in a dry atmosphere still resembles that of MoO_3, while the presence of water vapor induced significant structural changes. The structural information from the present EXAFS study is also consistent with previous Raman spectra, which clearly indicated the presence of MoO_3 after dry calcination and the formation of a surface heptamolybdate ($Mo_7O_{24}^{6-}$) in a humid atmosphere (*10*, *11*, *13*).

Interestingly, a new distance Mo–*X* was observed after thermal treatment which might be attributed to Mo–Al in a Mo–O–Al configuration, and if this could be confirmed, it would indicate the formation of anchoring bonds between the molybdenum oxide or molybdate species and the alumina surface.

ACKNOWLEDGMENTS

The work done in Munich was financially supported by the Deutsche Forschungsgemeinschaft, the Fonds der Chemischen Industrie, and by the Bundesminister für Forschung und Technologie.

REFERENCES

1. Knözinger, H., *in* "Proceedings, 9th International Congress on Catalysis, Calgary, 1988" (M. J. Phillips and M. Ternan, Eds.), Vol. 5, p. 20. Chem Institute of Canada, Ottawa, 1989; and references therein.
2. Liu, Y., Xie, Y., Li, C., Zou, Z., and Tang, Y., *J Catal. (China)* **5**, 234 (1984).

3. Xie, Y., Gui, L., Liu, Y., Zhao, B., Yang, N., Zhang, Y., Guo, Q., Duan, L., Huang, H., Cai, X., and Tang, Y., *in* "Proceedings, 8th International Congress on Catalysis, Berlin, 1984," Vol. 5, p. 147. Dechema, Frankfurt-am-Main, 1984.
4. Xie, Y., Gui, L., Liu, Y., Zhang, Y., Zhao, B., Yang, N., Guo, Q., Duan, L., Huang, H., Cai, X., and Tang, Y., *in* "Adsorption and Catalysis on Oxide Surfaces" (M. Che and G. C. Bond, Eds.), p. 139. Elsevier, Amsterdam, 1985.
5. Stampfl, S. R., Xa Chen, Dumesic, J. A., Niu, C., and Hill, Jr., C. G., *J. Catal.* **105,** 445 (1987).
6. Haber, J., *Pure Appl. Chem.* **56,** 1663 (1984).
7. Haber, J., Machej, T., and Czeppe, T., *Surf. Sci.* **151,** 301 (1985).
8. Bak, T., and Ziółkowski, J., *Bull. Acad. Polon. Sci. Ser. Sci. Chim.* **22,** 333 (1974).
9. Ziółkowski, J., Kozłowski, R., Mocała, K., and Haber, J., *J. Solid State Chem.* **35,** 297 (1980).
10. Leyrer, J., Zaki, M. I., and Knözinger, H., *J. Phys. Chem.* **90,** 4775 (1986).
11. Margraf, R., Leyrer, J., Knözinger, H., and Taglauer, E., *Surf. Sci.* **189/190,** 842 (1987).
12. Margraf, R., Leyrer, J., Taglauer, E., and Knözinger, H., *React. Kinet. Catal. Lett.* **35,** 261 (1987).
13. Leyrer, J., Margraf, R., Taglauer, E., and Knözinger, H., *Surf. Sci.* **201,** 603 (1988).
14. Korányi, T. I., Paál, Z., Leyrer, J., and Knözinger, H., *Appl. Catal.* **64,** L5 (1990).
15. Leyrer, J., Mey, D., and Knözinger, H., *J. Catal.* **124,** 349 (1990).
16. Dickinson, R. G., and Pauling, L., *J. Am. Chem. Soc.* **45,** 1455 (1923).
17. Matsumoto, K., Kobayashi, A., and Sasaki, Y., *Bull. Chem. Soc. Jpn.* **48,** 1009 (1975).
18. van Zon, J. B. A. D., Koningsberger, D. C., van't Blik, H. F. J., and Sayers, D. E., *J. Chem. Phys.* **82,** 5742 (1985).
19. *Struct. Rep.* **32A,** 296 (1967).
20. Kihlborg, L., *Ark. Kemi* **21,** 357 (1963).
21. Eisenberger, P., and Brown, G. S., *Solid State Commun.* **29,** 481 (1979).
22. Chiu, N.-S., Bauer, S. H., and Johnson, M. F. L., *J. Catal.* **89,** 226 (1984).
23. Leyrer, J., and Knözinger, H., unpublished results.
24. Harrison, W. T. A., Cheetham, A. K., and Faber Jr., J., *J. Solid State Chem.* **76,** 328 (1988).
25. McKale, A. G., Veal, B. W., Paulikas, A. P., Chan, S.-K., and Knapp, G. S., *J. Am. Chem. Soc.* **110,** 3763 (1988).